Journal of Molecular Structure 1277 (2023) 134833

Contents lists available at ScienceDirect

Journal of Molecular Structure

journal homepage: www.elsevier.com/locate/molstr

Experimental and density functional theoretical analyses on degradation of acid orange 7 via UV irradiation and ultrasound enhanced by fenton process

Sayiter Yildiz [a,*], Gamze Topal Canbaz [b], Savaş Kaya [c], Mikhail M. Maslov [d]

[a] Sivas Cumhuriyet University, Engineering Faculty, Department of Environmental Engineering, 58140, Sivas, Turkey
[b] Sivas Cumhuriyet University, Engineering Faculty, Department of Chemical Engineering, 58140, Sivas, Turkey
[c] Sivas Cumhuriyet University, Health Services Vocational School, Department of Pharmacy, 58140, Sivas, Turkey
[d] National Research Nuclear University "MEPhI", Department of Condensed Matter Physics, Kashirskoe Shosse 31, Moscow 115409, Russia

ARTICLE INFO

Article history:
Received 23 November 2022
Revised 14 December 2022
Accepted 19 December 2022
Available online 20 December 2022

Keywords:
Fenton-like reaction
DFT calculations
Degradation
OH radical

ABSTRACT

In this study, Acid Orange 7 (AO7) removal from synthetic water by advanced oxidation processes was investigated. Within the scope of the study, individual and different integrated applications of Fenton reaction, photooxidation and sonication were examined. The effects of variables such as H_2O_2, Fe^{2+}, reaction time, pH and initial dye concentration on the removal performance were investigated. Three different UV light sources, namely UV-A, UV-B and UV-C, were used. In order to study the effect of ultrasound addition, ultrasound with a frequency of 40 kHz and a power of 180 W was used. Effective AO7 degradation was achieved by Fenton oxidation at optimum conditions of 100 mg L^{-1} H_2O_2, 25 mg L^{-1} Fe^{2+}, 100 mg L^{-1} dye concentration, 3 pH and 30 min. The removal efficiency of the Fenton process was 97.6%, while it was for Fenton/UV-A, UV-B and UV-C light 97.6%, 96.97% and 97.35%, respectively. In the Fenton/US/UV process with ultrasound addition, removal efficiencies of 97.45%, 97.52% and 95.95% were obtained in UV-A, UV-B and UV-C lights, respectively. In Fenton/US process, the removal efficiency was 96.35%. In addition, in the kinetic study, it was determined that each process complied with the zeroth-order kinetics with the highest R^2 values. This study is especially important in terms of demonstrating the synergistic effect of these processes in an integrated reactor. Moreover, in such studies, the chemical reactivity analysis of the studied dye is quite important. For this aim, Density Functional Theory (DFT) calculations were performed. The study showed that Fenton processes can be used as an efficient and reliable method for AO7 removal. In this study, the experimental results for AO7 degradation were supported by theoretical calculations.

1. Inroduction

Azo dyes account for approximately 50% of the worldwide dyestuff production [1]. Its main applications are dyeing wool, silk and synthetic polyamide fibers [2]. More than 50% of textile waste contains azo dyes with -*N* = *N*- bonds [3]. Since the related dyeing process takes place in weakly acidic solution (pH 2–6), the term acid dye is often used [2].

Acid Orange 7 (AO7) is a long known and inexpensive azo dye. Like many other azo dyes, it tends to end up in industrial wastewater and poses a serious health threat to humans. It is highly toxic and may cause irritation to eyes, skin, mucous membranes and upper respiratory tract. In addition, it may have effects such as severe headache, nausea, water-borne diseases such as dermatitis and bone marrow loss leading to anemia [4]. Fig. 1 shows the chemical structure of the AO7 dye [5].

The properties of dye wastewater such as chemical structure and resistance to light and chemical attack make them highly resistant to microbial degradation [6]. Therefore, biological treatment processes are ineffective in removing these dyes from wastewater [7]. More powerful techniques are needed to treat dye-contaminated wastewater [8]. Many advanced oxidation processes (AOPs) are used to convert stubborn pollutants into biodegradable compounds. From these processes there are the Fenton reaction [9], direct ozonation [10], UV/hydrogen peroxide (H_2O_2) [11], and UV/photocatalyst [12]. Fenton reaction using ferrous ions (Fe^{2+}) and hydrogen peroxide (H_2O_2) is suitable for treating organic pollutants under acidic conditions with dual functions of oxidation and coagulation [13–14].

* Corresponding author.
E-mail address: sayiteryildiz@gmail.com (S. Yildiz).

https://doi.org/10.1016/j.molstruc.2022.134833
0022-2860/

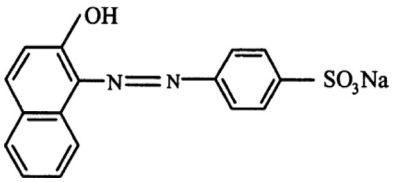

Fig 1. Chemical structure of AO7.

Physico-chemical methods such as adsorption, coagulation-flocculation can be very effective in removing color from wastewater [15]. Adsorption removal of AO7 is considered a simple and economical method for its removal from water and wastewater. Many studies have been carried out to reduce the AO 7 concentration by adsorption [16–17]. In addition, methods such as electrochemical oxidation [18], Wood-based biochar [19], Anaerobic treatment [5], electro-Fenton process [20], ultrasound [21], and Photocatalytic degradation [22] were investigated for AO7 removal. An integrated system using ultraviolet light (UV) and ultrasonic irradiation (US) in conjunction with Fenton has been studied in recent years as a promising way to degrade pollution from water and wastewater [23–24].

The 'Fenton reagent' is a mixture of hydrogen peroxide and divalent iron salts (Fe^{2+}/ H_2O_2), an effective oxidant for a wide variety of organic compounds. The effects of reactive amounts of $Fe^{2+}$and H_2O_2, the dosage ratio of H_2O_2 to Fe^{2+} (H_2O_2/ Fe^{2+}) or other factors on organic degradation have been extensively investigated in previous studies on the Fenton reaction [25–28]. During the degradation of H_2O_2 catalyzed by iron salts, hydroxyl radicals (OH•) are formed (Eq (1)) [29]. The production of OH• does not involve the use of harmful chemical reagents that can be harmful to the environment. So the process is environmentally friendly for wastewater treatment and looks promising for the treatment of water contaminated [30].

$$Fe^{2+} + H_2O_2 \rightarrow Fe^{3+} + OH\bullet + OH^- \quad (1)$$

However, a disadvantage of the method is that the oxidative activity of the Fe^{2+}/ H_2O_2 system is significantly reduced when the divalent iron becomes trivalent. Large amounts of sludge are also formed from the precipitation of iron. If the trivalent iron is converted back to the divalent state by light radiation (UV/VIS), the efficiency and effectiveness of the previous method can be increased significantly (Eq (2)). The removal efficiency increases as a result of the use of light due to additional OH• formation [31–32].

$$Fe^{3+} + H_2O + hv\ (\lambda < 450\ nm) \rightarrow Fe^{2+} + OH\bullet + H^+ \quad (2)$$

pH, iron concentration and H_2O_2 concentration are the main factors affecting Photo-Fenton oxidation [33]. The Sono-Photo-Fenton process requires a low amount of iron salt compared to Fenton. This is of economic importance for Sono-Photo-Fenton. Sono-Photo-Fenton can be explained by Eqs. (3)-(6) [24].

$$OH\bullet + HO\bullet_2 \rightarrow H_2O + O_2 \quad (3)$$

$$HO\bullet_2 + HO\bullet_2 \rightarrow H_2O_2 + O_2 \quad (4)$$

By US,

$$H\bullet + H_2O_2 \rightarrow OH\bullet + H_2O \quad (5)$$

$$Fe^{3+} + H\bullet \rightarrow Fe^{2+} + H^+ \quad (6)$$

In this study, individual and different integrated applications of Fenton reaction, photooxidation and sonication in AO7 removal from synthetic water were investigated. The synergistic effects of each process along with the removal efficiency were also examined. To our knowledge, only a few articles have been published regarding the synergistic use of AOPs for color removal. The effects of variables such as the performance of the integrated system, H_2O_2, Fe^{2+}, reaction time, pH and initial dye concentration on the oxidation process were investigated. This study is especially important in terms of demonstrating the synergistic effect of these processes in an integrated reactor. Experiments were performed three times and the data presented are the mean values obtained in the experiments, standard deviation ($\leq$4%) and error bars are indicated in the figures.

Chemical reactivity analysis is the prediction the behavior of the atomic or molecular systems under certain conditions. For chemical reactivity analysis, Density Functional Theory (DFT) and its chemical reactivity related branch (CDFT) are widely preferred. Moreover, in this study, we highlighted the nature of the chemical interactions between studied chemicals using computational analyses.

2. Material and methods

2.1. Experimental study

$FeSO_4{\cdot}7H_2O$ (P 99%) and H_2O_2 (P 35%) stock solutions were used as Fenton reagents in the study. The pH of the solution was adjusted by adding 0.1 N NaOH and 0.1 N H_2SO_4. After adjusting the pH to the desired value, Fe^{2+} (as $FeSO_4{\cdot}7H_2O$) and H_2O_2 dosing were carried out, respectively. After H_2O_2 dosing, the reaction time was considered to have started. Experiments were carried out in 250 ml flasks with 100 ml liquid volume. Different wavelengths of UV-A (365 nm), UV-B (302 nm), UV-C (256 nm) light were used as UV source. A multi-parameter device (Adwa AD8000) was used for pH measurements.

All chemicals applied in this study were of analytical standard. AO7 with molecular formula C16H11N2NaO4S was provided by Fluka Cas (no: 633–96–5). AO7 is a widely used anionic mono-azo dye and was chosen as a model of the water-soluble phenyl-azo-naphthol dye due to its resistance to biodegradation [22]. The AO7 stock solution was prepared by dissolving 1 g of AO7 with deionized water in a 1 L measuring flask. To prepare 100 mg L^{-1} of AO7 sample, an appropriate amount of AO7 from the stock solution was diluted to 100 mL with deionized water. The color point of the dye solution was determined using the UV–Visible Scanning Spectrophotometer (Merck Spectroquant Pharo 300). Azo dye can be analyzed simply and fast in UV–Vis spectroscopy. This is due to the absorption properties of the azo dye both in the UV due to the benzene rings and in the visible spectrum due to the chromophore group (-*N* = N-) [34].

In the study, AO7 removal efficiencies were determined by applying Fenton reagents at different doses. While determining the reagent amount ranges, the amounts used in previous studies were taken into account [26,28]. The next experiment involved optimum Fenton reagents with simultaneous use of UV irradiation. Finally, the effect of more simultaneous removal by three methods was investigated by applying ultrasound at a frequency of 40 kHz and a power of 180 W. The study was carried out in a custom-built reactor (Fig. 2).

The AO7 decolorization efficiency was calculated according to Eq. (7).

$$\text{Decolorization efficiency } \% = \left(1 - \frac{C}{C_0}\right) \times 100 \quad (7)$$

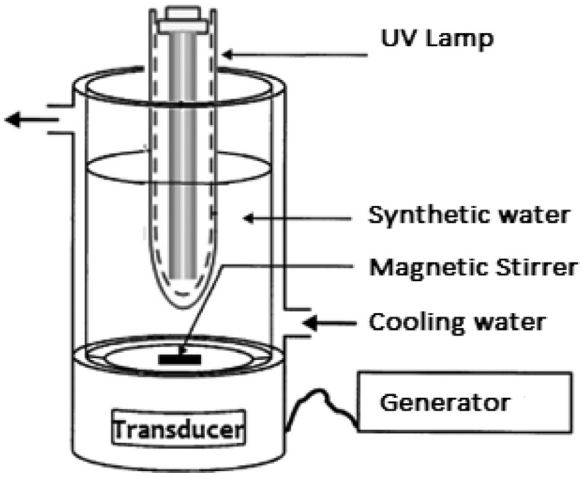

Fig 2. Schematic view of sono-photo-Fenton reactor.

Here; C_0 is the initial concentration of AO7 (mg L^{-1}) and C is the concentration of AO7 at reaction time t (min) (mg L^{-1}).

2.2. Details of density functional theory calculations

All calculations were performed using the Perdew-Burke-Ernzerhof (GGA-PBE) exchange-correlation functional [35] and hybrid electronic basis set combining 6–31G(d) [36] for elements Na, C, N, H, S, O and the 6–31G*-LDZ [37] for Fe. We used the graphics processor-based TeraChem software [38–41]. Geometry optimization was carried out with the efficient geomeTRIC energy minimizer [42]. The dispersion corrections D3 proposed by Grimme [43] were also included to take into account the weak non-covalent interactions. Conceptual Density Functional Theory (CDFT) is one of the popular theoretical tools used in local and global reactivities of the molecular systems. Conceptual DFT presents the following mathematical relations for chemical potential (μ), electronegativity (χ), hardness (η) and softness (σ). These relations have been derived from the parabolic relation with total number of the electrons of total electronic energy (E) [44].

$$\mu = -\chi = \left[\frac{\partial E}{\partial N}\right]_{v(r)} \tag{8}$$

$$\eta = \left[\frac{\partial \mu}{\partial N}\right]_{v(r)} = \left[\frac{\partial^2 E}{\partial N^2}\right]_{v(r)} \tag{9}$$

$$\sigma = 1/\eta$$

Using the finite differences approach, for the calculation of the aforementioned chemical descriptors, one can obtain the following formulae based on ionization energy and electron affinities calculated at ground state [45].

$$\mu = -\chi = -\left(\frac{I+A}{2}\right) \tag{10}$$

$$\eta = I - A \tag{11}$$

$$\sigma = 1/(I-A) \tag{12}$$

In especially organic chemistry, nucleophile and electrophile concepts found important applications in the estimation of reaction mechanisms and binding regions of molecules. In 1999, Parr, Szentpaly and Liu derived the electrophilicity index (ω) as [46–47]:

$$\omega = \chi^2/2\eta = \mu^2/2\eta \tag{13}$$

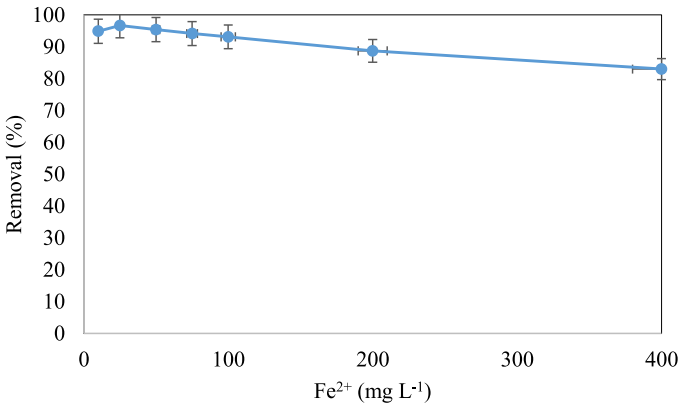

Fig. 3. Effect of Fe^{2+} dosage on the AO7 degratation.

The following parameters called as electrodonating power (ω^-) and electroaccepting power (ω^+) derived by Gazquez and his team [48] provides important clues about the electron donating and electron accepting capabilities of atomic and molecular systems

$$\omega^- = (3I+A)^2/(16(I-A)) \tag{14}$$

$$\omega^+ = (I+3A)^2/(16(I-A)) \tag{15}$$

Conceptual Density Functional parameters are widely taken into consideration in the studies regarding to the dye degradation because degradation process is closely related to the chemical reactivity of the studied dye.

3. Result and discussion

3.1. Effect of Fe^{2+} concentration

The effect of different concentrations of Fe^{2+} (10, 25, 50, 75, 100, 200, 400 mg L^{-1}) was investigated with constant values of dye concentration 100 mg L^{-1}, H_2O_2 100 mg L^{-1}, time (t) 30 min and pH 3 (Fig. 3). The dye removal efficiency was determined as 96.68% at the Fe^{2+}ion concentration of 25 mg L^{-1}. This result is due to the increase in hydroxyl radical production, which can improve the biodegradation of the dye [49]. However, with increasing Fe^{2+}concentration, AO7 removal efficiency decreased. It decreased to 82.99% with Fe^{2+}concentration of 400 mg L^{-1}. This is because, due to the combination of the iron ion with the hydroxyl radical, the hydroxyl radicals are more inaccessible with a further increase in $Fe^{2+}$and the dye removal efficiency by the hydroxyl radicals decreases [50]. This situation has also been reported in different studies [51–52].

In general, the degradation of organics increases with increasing Fe^{2+} dosage. However, excess Fe^{2+} can compete with organics for OH• (Eq (16)) and leads to a reduction in the degradation efficiency [53]. Competitive effects can also occur in the presence of excessive H_2O_2 (Eq (17)). Therefore, the dosage rate is commonly taken as an operating parameter in the Fenton reaction, according to the OH• competition between $Fe^{2+}$and H_2O_2 [54].

$$Fe^{2+} + \bullet OH \rightarrow Fe^{3+} + OH^- \tag{16}$$

$$H_2O_2 + \bullet OH \rightarrow HO_2\bullet/O_2\bullet^- + H_2O \tag{17}$$

3.2. Effect of addition of hydrogen peroxide

The results of the degradation of AO7 (100 mg L^{-1}) using different concentrations of H_2O_2 (10, 25, 50, 75, 100, 150, 200, 300,

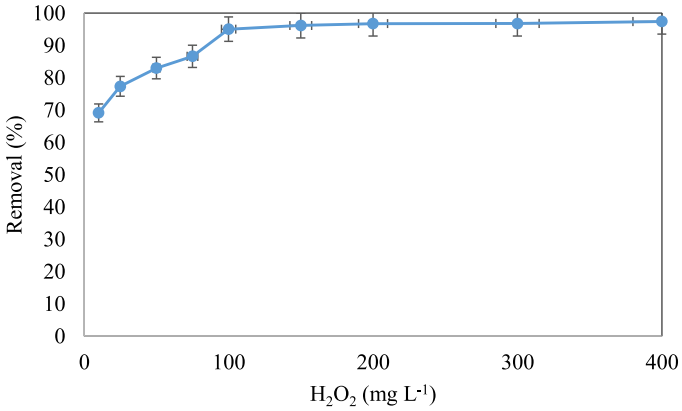

Fig. 4. Effect of H_2O_2 dosage on the AO7 degratation.

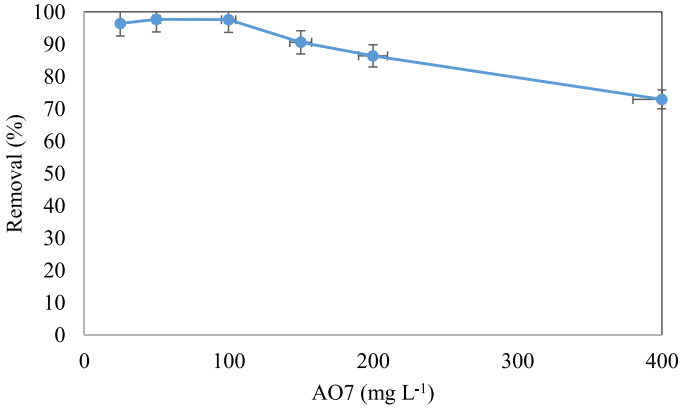

Fig. 5. Effect of AO7 concentraiton on degratation.

400, 500) are given in Fig. 4. The study was carried out under Fe^{2+} 50 mg L^{-1}, t 30 min and pH 3 constant conditions. The removal efficiency increased with increasing H_2O_2, but the improvement was not evident above 150 mg L^{-1}.

Since H_2O_2 is the source of OH• radicals formed by the Fenton reaction, the process performance improves when the amount of H_2O_2 is increased up to a certain value. The fact that the amount of H_2O_2 increases further and moves away from the optimum level both increases the cost of the process and leads to the formation of HO_2• (Eq (18)) with lower oxidation power by reacting between excess H_2O_2 and OH• [55].

$$H_2O_2 + OH^{\bullet} \rightarrow H_2O + HO_2\bullet \quad (18)$$

As seen in Fig. 4, while the dye removal efficiency was 69.13% in the use of 10 mg L^{-1} H_2O_2, it was determined as 95.04% in 100 mg L^{-1} H_2O_2 and 97.17% in 500 mg L^{-1} H_2O_2. There was no significant change in the removal efficiency in the use of H_2O_2 over 100 mg L^{-1}.

3.3. Effect of initial AO7 concentration

From a practical standpoint, it is important to examine the dependence of the removal efficiency on the initial concentration of the dye. The efficiency of dye removal using the Fenton process was investigated by varying the concentration of AO7 at a constant values of 25 mg L^{-1} Fe^{2+}, 100 mg L^{-1} H_2O_2, t 30 min, and pH 3 (Fig. 5). Increasing the concentration of pollutants can reduce the removal efficiency of pollutants [56].

In Fig. 5, it is seen that the color removal efficiency decreases as the initial dye concentration increases. While the removal efficiency was 97.8% at the initial concentration of 50 mg L^{-1}, it decreased to 86.4% and 72.9% at 200 and 400 mg L^{-1} concentrations, respectively. This is due to the constant OH• radicals in solution despite the increasing concentration of the dye molecule. In this case, more radical consumption occurs during the oxidation process [57]. The decrease in removal efficiency with increasing dye concentration has been reported by different researchers [58–59].

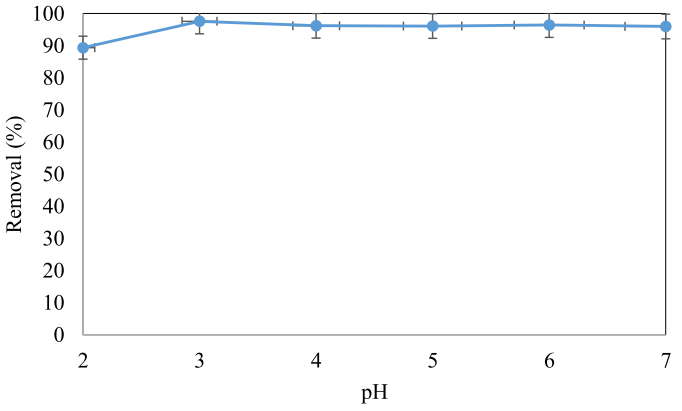

Fig. 6. Effect of H_2O_2 dosage on the AO7 degratation.

3.4. Effect of the initial pH

To determine the effect of pH on the degradation efficiency of AO7, the pH range of 2–7 was applied. Other parameters were constant as 25 mg L^{-1} Fe^{2+}, 100 mg L^{-1} H_2O_2, t 30 min and AO7 concentration 100 mg L^{-1}. The results showed that the pH of the solution had no direct significant effect on AO7 removal Fig. 6). Studies have reported that the most effective pH value for Fenton and Photo-Fenton processes is generally close to 3.0 [33]. In this study, while the removal efficiency was 89.3% at pH 2, the highest removal efficiency of 97.6% was obtained at pH 3. At lower pH, hydroxyl radicals are used by H^+ ions and the rate of removal decreases. Also, H_2O_2 is electro-fugitive and can take up a proton at low pH and convert to $H_3O_2^+$, which is a reason to reduce decolorization (Eqs. (19)-(20)) [60].

$$OH + H^+ + e^- \rightarrow H_2O \quad (19)$$

$$H_2O_2 + H^+ \rightarrow H_3O_2^+ \quad (20)$$

3.5. Effect of reaction time

The effect of the reaction time on the removal efficiency of AO7 was investigated at constant values of 25 mg L^{-1} Fe^{2+}, 100 mg L^{-1} H_2O_2, pH 3, AO7 concentration at 100 mg L^{-1} with different times (5, 10, 15, 20, 25, 30, 45, 60, 90, 120, 180, 240 min). According to the results, the most dye removal occurred in the first few minutes and did not show a significant change from the 15th minute (Fig. 7).

As seen in Fig. 8, the removal efficiency at the 30th minute of the reaction was 97.6%, while it was 97.61% and 97.96% at the 60th and 240 th minute, repectively. The short time required for degradation indicates the presence of easily degradable organic substances, while the opposite situation indicate the existence of hard-to-degrade organic substances [61].

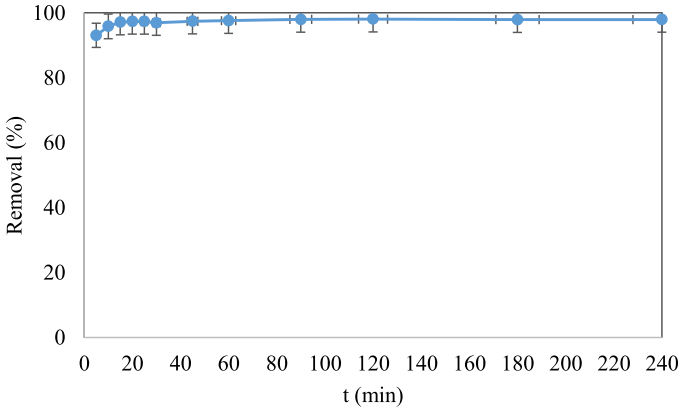

Fig. 7. Effect of reaction time on the AO7 degratation.

3.6. Photo fenton / sono-fenton/ sono-photo fenton

Photo Fenton (Fenton/UV), sono-Fenton (Fenton/US), and sono-photo-Fenton (Fenton/UV/US) degradation of AO7 were carried out at constant values of H_2O_2 (100 mg L^{-1}), Fe^{2+} (25 mg L^{-1}), and pH (3), which were determined in the first stage of this study. To investigate the properties of different processes; Fenton/UV (Fe^{2+}/H_2O_2/UV-A/UV-B/UV-C), Fenton/US (Fe^{2+}/ H_2O_2/US) and Fenton/US/UV (Fe^{2+}/ H_2O_2/US/ UV-A/UV-B/UV-C) was conducted to compare the individual and synergistic effects in a batch reactor. Fig. 8 shows the results demonstrating the dye removal efficiency for all methods.

As seen in Fig. 8, there was no significant change in AO7 removal efficiencies for different AOPs applications. In the Fenton application, high removal efficiencies were obtained in a very short time (97.6%) with the addition of reagents. This high removal efficiency reduced the effects that may occur as a result of the use of UV and US. The Fenton reaction produced very good results for AO7 removal even when used alone. The removal efficiency of UV-A, UV-B and UV-C lights in the photo Fenton process performed with different light sources was 97.6%, 96.97% and 97.35%, respectively. In the Fenton/US/UV process with ultrasound added, removal efficiencies of 97.45%, 97.52% and 95.95% were obtained for UV-A, UV-B, UV-C, respectively. In the Fenton/US process, the removal efficiency was 96.35%.

Table 1
Kinetic constants in Fenton processes.

Process	0th. Order Kinetic		1st. Order Kinetic		2nd. Order Kinetic	
	k_0 (mg L.min^{-1})	R^2	k_1 (1 min^{-1})	R^2	k_2 (L mg.min^{-1})	R^2
Fenton	0.1558	0.70	0.0016	0.70	−2E-05	0.69
Fenton/UV-A	0.1598	0.7	0.0016	0.72	−2E-05	0.71
Fenton/UV-B	0.1607	0.76	0.0017	0.75	−2E-05	0.75
Fenton/UV-C	0.1741	0.62	0.0018	0.61	−2E-05	0.61
Fenton/US	0.136	0.70	0.0014	0.70	−2E-05	0.69

3.7. Kinetic study

In this study, zeroth-order (Eq (21)), first-order (Eq (22)), and second-order (Eq (23)) kinetic models were tested to investigate the degradation of AO7 by different AOPs [27]. The obtained kinetic constants and R^2 values are given in Table 1.

$$C = C_0 - k_0.t \tag{21}$$

$$\ln C = \ln C_0 - k_1.t \tag{22}$$

$$\frac{1}{C} = \frac{1}{C_0} + k_2.t \tag{23}$$

Here; C_0 initial AO7 concentration (mg L^{-1}); C is the concentration of AO7 (mg L^{-1}) at any given time; k_0, k_1 and k_2 of the kinetics of the zeroth, first and second order reaction kinetic constants, respectively; and t represents reaction time (minutes).

As shown in Table 1, the R^2 values were very close for each process. However, it was determined that each application of the Fenton process fit the zeroth-order kinetics with the best R^2 values as a function of AO7 concentration. In the 2nd degree kinetic calculation, the k_2 coefficient could not be calculated because the values were too small. According to the Fenton process, a slight increase was observed in the k constants in the photo Fenton processes performed under UV light. While the k_0 value was 0.1558 in the Fenton process, it was calculated as 0.1598, 0.1607 and 0.1741

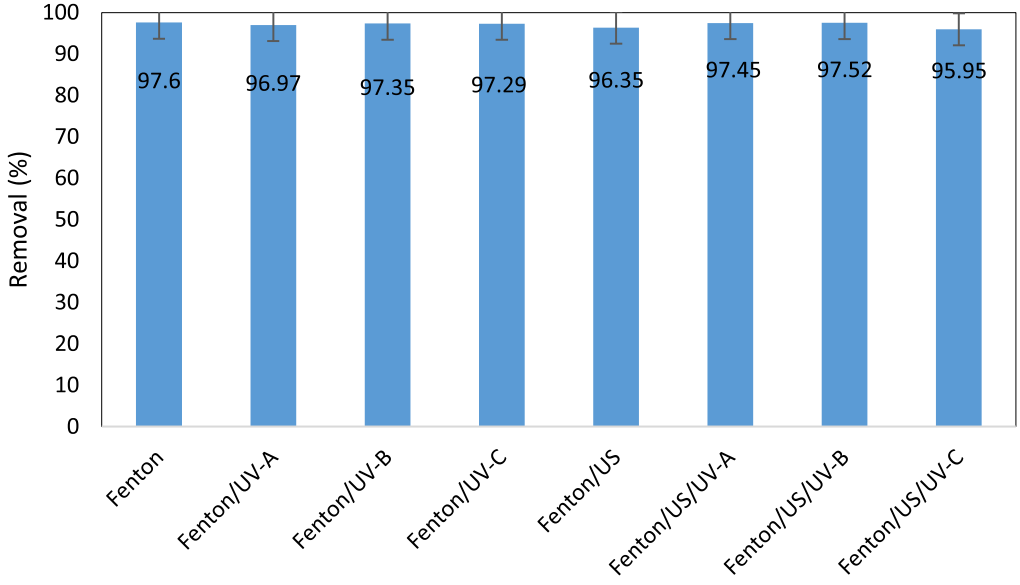

Fig. 8. Effect of different AOPs on the AO7 degratation.

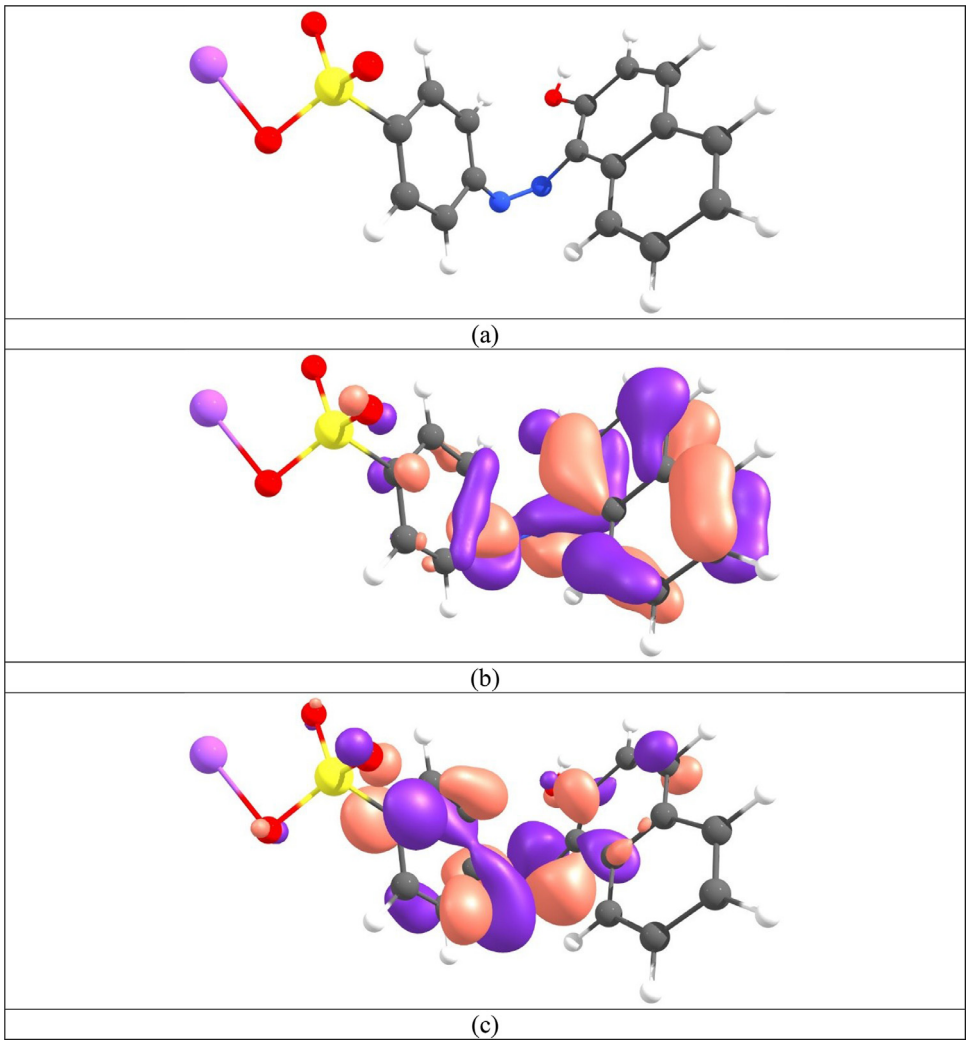

Fig. 9. AO7: atomic structure (a), HOMO (b), and LUMO (c).

Table 2
Calculated electronic characteristics as a result of interaction Fe^{2+} and H_2O_2 with AO7.

Name	Dipole moment (Debye)	HOMO (eV)	LUMO (eV)	η (eV)	χ (eV)	ω (eV)	ω^- (eV)	ω^+ (eV)	Binding Energy (eV)
AO7	6.932	−4.471	−2.672	1.799	3.57	3.54	8.98	5.41	–
AO7/Fe^{2+}	8.383	−11.342	−11.173	0.169	11.25	374.94	755.52	744.27	16.53
AO7/H_2O_2	7.017	−4.922	−2.982	1.940	3.95	4.02	10.14	6.19	1.43

in the UV-A, UV-B and UV-C processes, respectively. This can be explained by the relative increase in temperature with the use of UV light [62].

3.8. The result of DFT calculations

We analyzed the effect of the Fe^{2+} ion and H_2O_2 molecule on the geometry and electronic structure of the AO7. Both the Fe ion and the hydrogen peroxide molecule strongly distort the AO7 structure (see Figs. 1-3), which leads to further destruction. It can be seen that geometrically the ion is located exactly above the center of the six-membered ring, and the hydrogen peroxide molecule is located closer to the sodium atom, weakly binding to oxygen atoms. In addition, the presence of the ion significantly changes the electronic structure of AO7, facilitating charge transfer and significantly reducing the gap between the frontier orbitals (see Table 2). The binding energies of the Fe^{2+} and H_2O_2 were obtained according to the following formulae, respectively Eqs. (24)-(25).

$$E_b = E\left(Fe^{2+}\right) + E(AO7) - E\left(AO7/Fe^{2+}\right) \quad (24)$$

$$E_b = E(H_2O_2) + E(AO7) - E(AO7/H_2O_2) \quad (25)$$

The results show that the ion binds to AO7 much more strongly compared with the H_2O_2. The values of the corresponding binding energies are presented in Table 2.

Before the mentioning from the relation with chemical reactivity of the dyes studied of Fenton process, let us mention from popular electronic structure principles like Maximum Hardness Principle [63]. According to this principle, chemical hardness reported as the resistance towards electron cloud polarization of atomic and molecular systems is a good measure of the stability of molecules [64–65]. It should be reported that in stable states, chemical hardness is maximized. The inverse relation between hardness and

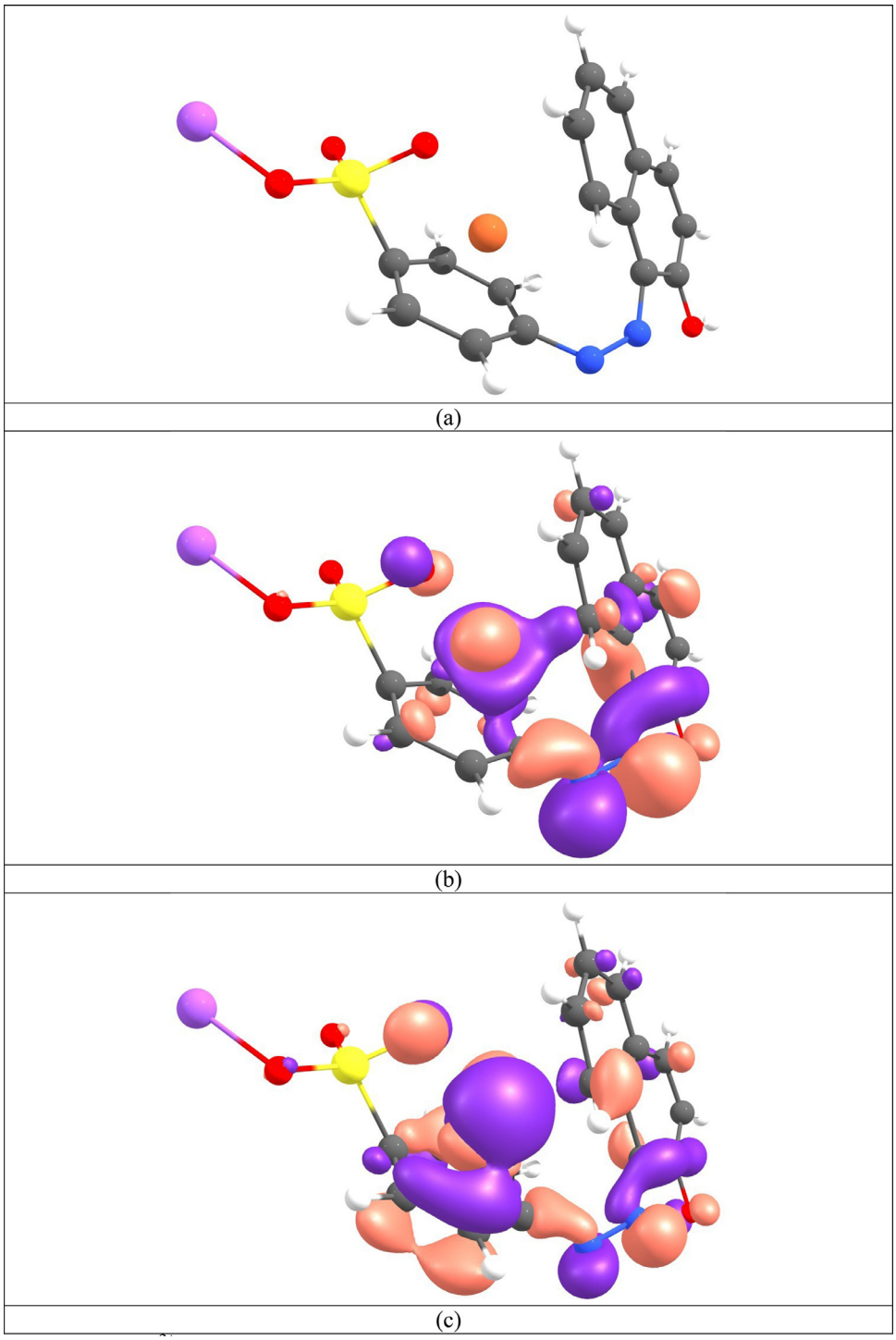

Fig. 10. AO7/Fe^{2+} complex: atomic structure (a), HOMO (b), and LUMO (c).

polarizability was highlighted by Ghanty and Ghosh [66]. If so, it is not difficult to predict that stable states correspond to the minimum value of the polarizability. Some researchers noted that dipole moment can be considered as a measure of the polarizability. According to Hard and Soft Acid-Base Principle (HSAB) [67] "hard acids prefer to coordinate to hard bases and soft acids prefer to coordinate to soft bases." It should be noted that Fenton process is quite useful to work the degradation of the dyes with low hardness and high polarizability, namely reactive dyes. From the calculated chemical hardness and dipole moment values, it can be reported that our dye AO7 is quite reactive and soft molecule. Some authors noted that OH radical acts as a good electron acceptor [68]. After the interaction with Fe^{2+}ion of AO7 dye, it is clear that chemical hardness of the system decreases, namely reactivity of the system increases. In this way, degradation of the reactive system with OH radical happens more easily. As a result, it can be said that the result of the theoretical analyses performed are in good agreement with experiments made. Figs. 9 and 11 visually presents the atomic structure, HOMOs and LUMOs of the calculated chemical systems. The binding energy calculated for the interaction with AO7 of Fe^{2+} is 16.53 eV. This interaction supports the HSAB Principle.

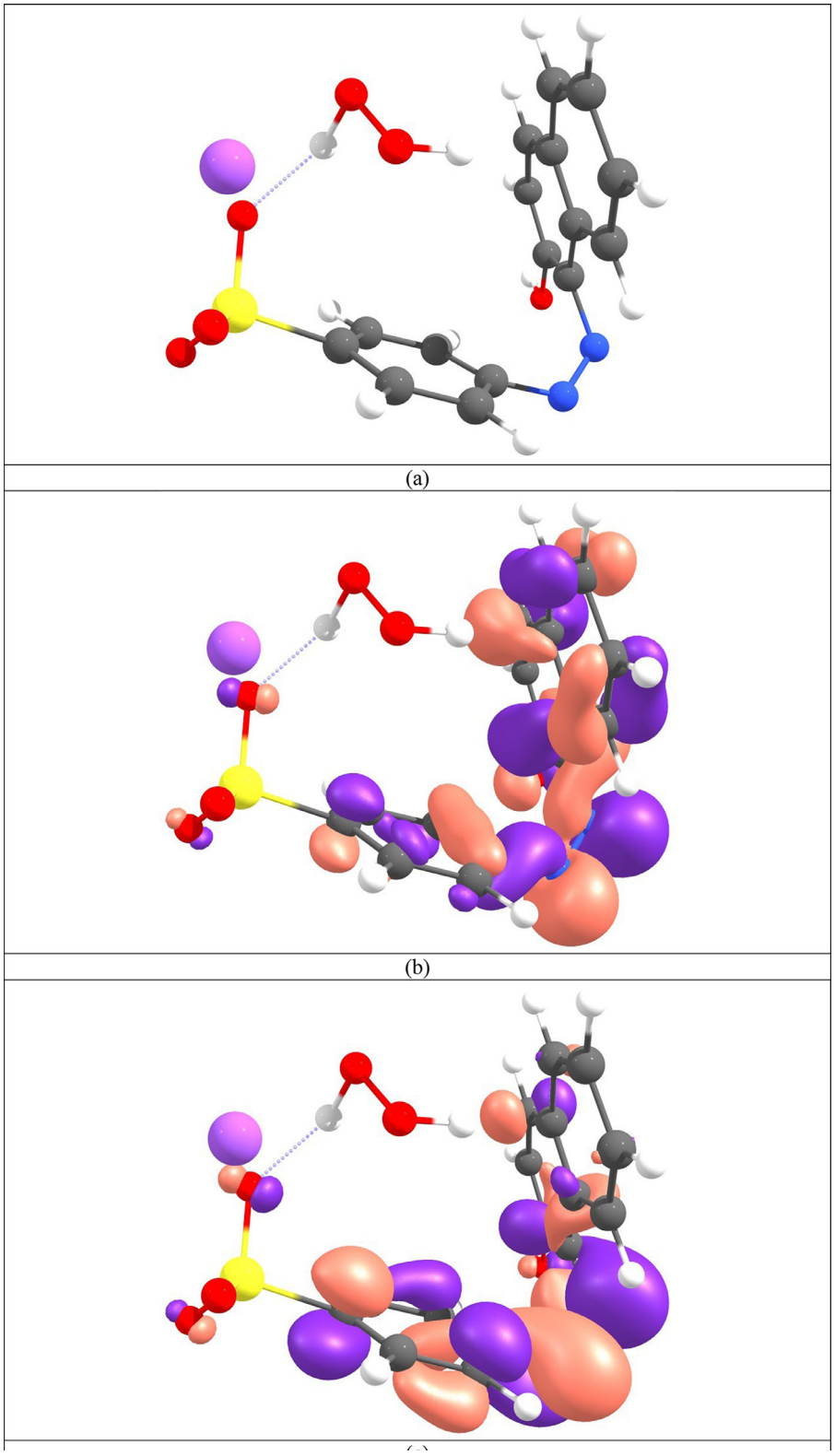

Fig. 11. AO7/H_2O_2 complex: atomic structure (a), HOMO (b), and LUMO (c).

4. Conclusion

In this study, the degradation of AO7 in aqueous solution was investigated by Fenton, photo-Fenton, sono-Fenton and sono-photo-Fenton processes under different experimental conditions. Color removal using the Fenton process was affected by the main variables such as pH, initial dye concentration, H_2O_2 dose, Fe^{2+} dose and reaction time. Effective AO7 degradation was achieved by Fenton oxidation at optimum conditions of 100 mg L- H_2O_2, 25 mg L^{-1} Fe^{2+}, 100 mg L^{-1} dye concentration, 3 pH and 30 min. Three

different light sources, namely UV-A, UV-B and UV-C, were used in the photo Fenton process. In addition, AO7 removal efficiencies were investigated by using Fenton and photo Fenton processes together with US source (Fenton/US and Fenton/UV/US). In addition, with the best R^2 values obtained in the kinetic study, it was determined that each process complied with the zeroth-order kinetics. Moreover in this study, the chemical reactivity analysis of the studied dye was performed. For this aim, DFT calculations were performed. Theoretical calculations supported the experimental observations. The results revealed that the Fenton-like process is a suitable process with high removal efficiency of AO7 removal from aqueous solutions. This process can be considered as a promising and effective method for removing dyes from water and wastewater.

Declaration of Competing Interest

The authors declare that they have no known competing financial interests or personal relationships that could have appeared to influence the work reported in this paper.

CRediT authorship contribution statement

Sayiter Yildiz: Methodology, Data curation, Validation, Writing – original draft, Supervision. **Gamze Topal Canbaz:** Resources, Data curation, Formal analysis. **Savaş Kaya:** Software, Writing – review & editing. **Mikhail M. Maslov:** Software, Formal analysis, Visualization.

Data availability

No data was used for the research described in the article.

References

[1] A. Szyguła, E. Guibal, M. Ruiz, A.M. Sastre, The removal of sulphonated azo-dyes by coagulation with chitosan, Colloids Surf. A 330 (2008) 219–226.
[2] V.K. Gupta, Application of low-cost adsorbents for dye removal–a review, J. Environ. Manag. 90 (8) (2009) 2313–2342.
[3] H. Chen, J. Motuzas, W. Martens, J.C. Diniz da Costa, Degradation of azo dye Orange II under dark ambient conditions by calcium strontium copper perovskite, Appl. Catal. B Environ. 221 (2018) 691–700.
[4] M. Greluk, Z. Hubicki, Efficient removal of Acid Orange 7 dye from water using the strongly basic anion exchange resin Amberlite IRA-958, Desalination 278 (1–3) (2011) 219–226.
[5] D. Mendez-Paz, F. Omil, J.M. Lema, Anaerobic treatment of azo dye Acid Orange 7 under fed-batch and continuous conditions, Water Res. 39 (5) (2005) 771–778.
[6] H.Y. Li, Y.L. Li, L.J. Xiang, Q.Q. Huang, J.J. Qiu, H. Zhang, M.V. Sivaiah, F. Baron, J. Barrault, S. Petit, S. Valange, Heterogeneous photo-Fenton decolorization of Orange II over Al-pillared Fe-smectite: response surface approach, degradation pathway, and toxicity evaluation, J. Hazard. Mater. 287 (2015) 32–41.
[7] H. Zhang, L.J. Duan, Y. Zhang, F. Wu, The use of ultrasound to enhance the decolorization of the C.I. Acid Orange 7 by zero-valent iron, Dyes Pigm. 65 (2005) 39–43.
[8] J. Li, H. Lin, K. Zhu, H. Zhang, Degradation of Acid Orange 7 using peroxymonosulfate catalyzed by granulated activated carbon and enhanced by electrolysis, Chemosphere 188 (2017) 139–147.
[9] T. Maezono, M. Tokumura, M. Sekine, Y. Kawase, Hydroxyl radical concentration profile in photo-Fenton oxidation process: generation and consumption of hydroxyl radicals during the discoloration of azo-dye Orange II, Chemosphere 82 (2011) 1422–1430.
[10] N.A. Medellin-Castillo, R. Ocampo-Perez, R. Leyva-Ramos, M. Sanchez-Polo, J. Rivera-Utrilla, J.D. Mendez-Díaz, Removal of diethyl phthalate from water solution by adsorption, photo-oxidation, ozonation and advanced oxidation process (UV/H_2O_2, O_3/H_2O_2 and O_3/activated carbon), Sci. Total Environ. 442 (2013) 26–35.
[11] Y. Lester, D. Avisar, H. Mamane, Photodegradation of the antibiotic sulphamethoxazole in water with UV/H_2O_2 advanced oxidation process, Environ. Technol. 31 (2010) 175–183.
[12] Y.S. Wang, J.H. Shen, J.J. Horng, Chromate enhanced visible light driven TiO_2 photocatalytic mechanism on Acid Orange 7 photodegradation, J. Hazard Mater. 274 (2014) 420–427.
[13] H. Wu, M.M. Fan, C.F. Li, M. Peng, L.J. Sheng, Q. Pan, G.W. Song, Kinetic studies on the degradation of crystal violet by the Fenton oxidation process, Water Sci. Technol. 62 (2010) 1–7.
[14] X. Cao, H. Lou, W. Wei, L. Zhu, Treatment of tetrahydrofuran wastewater by the Fenton process: response surface methodology as an optimization tool, Water Sci. Technol. 69 (2014) 1080–1087.
[15] J. Sarasa, M.P. Roche, M.P. Ormad, E. Gimeno, A. Puig, J.L. Ovelleiro, Treatment of a wastewater resulting from dyes manufacturingwith ozone and chemical coagulation, Water Res. 32 (9) (1998) 2721–2727.
[16] V.K. Gupta, R. Jain, S. Varshney, Removal of Reactofix golden yellow 3 RFN from aqueous solution using wheat husk an agricultural waste, J. Hazard. Mater. 142 (2007) 443–448.
[17] V.K. Gupta, A. Mittal, V. Gajbe, J. Mittal, Removal and recovery of the hazardous azo dye Acid Orange 7 through adsorption over waste materials: bottom ash and de-oiled soya, Ind. Eng. Chem. Res. 45 (2006) 1446–1453.
[18] A. Fernandes, A. Morao, M. Magrinho, A. Lopes, I. Goncalves, Electrochemical degradation of CI Acid Orange 7, Dyes and Pigments 61 (3) (2004) 287–296.
[19] K. Zhu, X. Wang, D. Chen, W. Ren, H. Lin, H. Zhang, Wood-based biochar as an excellent activator of peroxydisulfate for Acid Orange 7 decolorization, Chemosphere 231 (2019) 32–40.
[20] B. Ramírez-Pereda, A. Álvarez-Gallegos, J.G. Rangel-Peraza, Y.A. Bustos-Terrones, Kinetics of Acid Orange 7 oxidation by using carbon fiber and reticulated vitreous carbon in an electro-Fenton process, J. Environ. Manag. 213 (2018) 279–287.
[21] F. Liu, P. Yi, X. Wang, H. Gao, H. Zhang, Degradation of Acid Orange 7 by an ultrasound/ZnO-GAC/persulfate process, Sep. and Pur. Techno. 194 (2018) 181–187.
[22] F. Han, V.S.R. Kambala, R. Dharmarajan, Y. Liu, R. Naidu, Photocatalytic degradation of azo dye acid orange 7 using different light sources over Fe^{3+} doped TiO_2 nanocatalysts, Environ. Techno. & Innov. 12 (2018) 27–42.
[23] L.J. Xu, W. Chu, N. Graham, Degradation of di-n-butyl phthalate by a homogeneous sono–photo-Fenton process with in situ generated hydrogen peroxide, Chem. Eng. J. 240 (2014) 541–547.
[24] P. Vaishnave, A. Kumar, R. Ameta, P.B. Punjabi, S.C. Ameta, Photo oxidative degradation of azure-B by sono–photo-Fenton and photo-Fenton reagents, Arabian J. Chem. 7 (2014) 981–985.
[25] M.S.F. Santos, A. Alves, L.M. Madeira, Paraquat removal from water by oxidation with Fenton's reagent, Chem. Eng. J. 175 (2011) 279–290.
[26] S. Yildiz, A. Olabi, Effect of Fe^{2+} and Fe^0 Applied Photo-Fenton Processes on Sludge Disintegration, Chem. Eng. Tech. 44 (1) (2021) 95–103.
[27] A. Olabi, S. Yildiz, Sludge disintegration using UV assisted Sono-Fenton process, Environ. Sci. and Poll. Res. 28 (2021) 52565–52575.
[28] S. Yildiz, A. Cömert, Fenton process effect on sludge disintegration, Int. J. Environ. Health Res. 30 (1) (2020) 89–104.
[29] N. Jaafarzadeh, A. Takdastan, S. Jorfi, F. Ghanbari, M. Ahmadi, G. Barzegar, The performance study on ultrasonic/Fe_3O_4/H_2O_2 for degradation of azo dye and real textile wastewater treatment, J. Mol. Liq. 256 (2018) 462–470.
[30] I. Sirés, J.A. Garrido, R.M. Rodríguez, E. Brillas, N. Oturan, M.A. Oturan, Catalytic behavior of the Fe^{3+}/Fe^{2+} system in the electro-Fenton degradation of the antimicrobial chlorophene, Appl. Catal. B: Environ. 72 (3/4) (2007) 382–394.
[31] M.H. Zhang, H. Dong, L. Zhao, D.X. Wang, D. Meng, A review on Fenton process for organic wastewater treatment based on optimization perspective, Sci. Total Environ. 670 (2019) 110–121.
[32] M.S. Lucas, J.A. Peres, Decolorization of the azo dye Reactive Black 5 by Fenton and photo-Fenton oxidation, Dyes and Pigments 71 (3) (2006) 236–244.
[33] L.C. Almeida, S. Garcia-Segura, C. Arias, N. Bocchi, E. Brillas, Electrochemical mineralization of the azo dye Acid Red 29 (Chromotrope 2R) by photoelectro-Fenton process, Chemosphere 89 (6) (2012) 751–758.
[34] A. Maroudas, P.K. Pandis, A. Chatzopoulou, L.R. Davellas, G. Sourkouni, C. Argirusis, Synergetic decolorization of azo dyes using ultrasounds, photocatalysis and photo-fenton reaction, Ultrason. Sonochem. 71 (2021) 105367.
[35] J.P. Perdew, K. Burke, M. Ernzerhof, Generalized Gradient approximation made simple, Phys. Rev. Lett. 77 (1996) 3865–3868.
[36] W.J. Hehre, R. Ditchfield, J.A. Pople, Self-consistent molecular orbital methods. XII. Further extensions of Gaussian-type basis sets for use in molecular orbital studies of organic molecules, J. of Chem. Phys. 56 (5) (1972) 2257–2261.
[37] P.J. Hay, W.R. Wadt, Ab initio effective core potentials for molecular calculations. Potentials for K to Au including the outermost core orbitals, J. of Chem. Phys 82 (1985) 299–310.
[38] I.S. Ufimtsev, T.J. Martínez, Quantum chemistry on graphical processing units. 3. analytical energy gradients and first principles molecular dynamics, J. Chem. Theo. Comp. 5 (2009) 2619–2628.
[39] A.V. Titov, I.S. Ufimtsev, N. Luehr, T.J. Martínez, Generating efficient quantum chemistry codes for novel architectures, J. Chem. Theo. Comp. 9 (2013) 213–221.
[40] J. Kästner, J.M. Carr, T.W. Keal, W. Thiel, A. Wander, P. Sherwood, DL-FIND: an OpenSource Geometry Optimizer for Atomistic Simulations, J. Phys. Chem. A 113 (43) (2009) 11856–11865.
[41] T.P.M. Goumans, C.R.A. Catlow, W.A. Brown, J. Kästner, P. Sherwood, An Embedded Cluster Study of the Formation of Water on Interstellar Dust Grains, Phys. Chem. Chem. Phys. 11 (26) (2009) 5431–5436.
[42] L.P. Wang, C. Song, Geometry optimization made simple with translation and rotation coordinates, J. Chem. Phys. 144 (21) (2016) 214108.
[43] S. Grimme, J. Antony, S. Ehrlich, H. Krieg, A consistent and accurate ab initio parametrization of density functional dispersion correction (DFT-D) for the 94 elements H-Pu, J. Chem. Phys. 132 (15) (2010) 154104.
[44] N. Islam, S. Kaya (Eds.), Conceptual Density Functional Theory and Its Application in the Chemical Domain, CRC Press, 2018.

[45] S. Kaya, P. Banerjee, S.K. Saha, B. Tüzün, C. Kaya, Theoretical evaluation of some benzotriazole and phospono derivatives as aluminum corrosion inhibitors: DFT and molecular dynamics simulation approaches, RSC Adv. 6 (78) (2016) 74550–74559.
[46] R.G. Parr, L.V. Szentpály, S. Liu, Electrophilicity index, J. of the American Chem. Soc. 121 (9) (1999) 1922–1924.
[47] L. von Szentpály, S. Kaya, N. Karakuş, Why and when is electrophilicity minimized? New theorems and guiding rules, J of Phy. Chem. A 124 (51) (2020) 10897–10908.
[48] J.L. Gázquez, A. Cedillo, A. Vela, Electrodonating and electroaccepting powers, J of Phy. Chem. A 111 (10) (2007) 1966–1970.
[49] J.Y. Feng, X.J. Hu, P.L. Yue, H.Y. Zhu, G.Q. Lu, Discoloration and mineralization of Reactive Red HE-3B by heterogeneous photo- Fenton reaction, Water Res. 37 (2003) 3776–3784.
[50] C. Özdemir, M.K. Öden, S. Şahinkaya, E. Kalipçi, Color removal from synthetic textile wastewater by sono-Fenton process, CLEAN - Soil Air Water 39 (2011) 60–67.
[51] H. Katsumata, T. Kobayashi, S. Kaneco, T. Suzuki, K. Ohta, Degradation of linuron by ultrasound combined with photo- Fenton treatment, Chem. Eng. J. 166 (2011) 468–473.
[52] Y. Yosofi, S.A. Mousavi, Sono-photo-Fenton degradation of Reactive Black 5 from aqueous solutions: performance and kinetics. Desalin, and Water Treat 174 (2020) 354–360.
[53] H. Hayashi, Y. Nakajima, K. Ohta, Novel degradation method of organic compounds in human surroundings using iron oxide, Rep. Technol. Res. Inst. Osaka. Pref. 21 (2007) 79–83.
[54] J.H. Shen, J.J. Horng, Y.S. Wang, Y.R. Zeng, The use of reactive index of hydroxyl radicals to investigate the degradation of acid orange 7 by Fenton process, Chemosphere 182 (2017) 364–372.
[55] A. Nikravan, Amoxicillin and Ampicillin Removal from Wastewater by Fenton and Photo-Fenton Processes, Hacettepe university, Ankara, Turkey, 2015 Master thesis. Department of environmental engineering.
[56] P.N. Patil, P.R. Gogate, Degradation of methyl parathion using hydrodynamic cavitation: effect of operating parameters and intensification using additives, Sep. Purif. Technol. 95 (2012) 172–179.
[57] X. Zhong, S. Royer, H. Zhang, Q.Q. Huang, L.J. Xiang, S. Valange, J. Barrault, Mesoporous silica iron-doped as stable and efficient heterogeneous catalyst for the degradation of C.I. Acid Orange 7 using sono–photo-Fenton process, Sep. Purif. Technol. 80 (2011) 163–171.
[58] G. Harichandran, S. Prasad, SonoFenton degradation of an azo dye, Direct Red, Ultrason. Sonochem. 29 (2016) 178–185.
[59] M. Dehghani, S. Shahsavani, F. Jamshidi, N. Shamsedini, Comparison the efficiency of Fenton and Photo–fenton processes for the removal of Reactive red 198 Dye from the aqueous solution, Iranian J. Health Safety and Environ. 6 (4) (2020) 1336–1342.
[60] B. Neppolian, H.Y. Jung, H.C. Choi, J.H. Lee, J.W. Kang, Sonolytic degradation of methyl tert-butyl ether: the role of coupled Fenton process and persulphate ion, Water Res. 36 (2002) 4699–4708.
[61] S. Parsons, Advanced Oxidation Processes For Water and Wastewater Treatment, IWA publishing, 2004.
[62] J.C. Kotz, P.M. Treichel, J. Townsend, Chemistry and chemical reactivity, 8th edition. Cengage Learning. ISBN 9780840048288. View at: google Books, (2012).
[63] S. Kaya, C. Kaya, A simple method for the calculation of lattice energies of inorganic ionic crystals based on the chemical hardness, Inorg. Chem. 54 (17) (2015) 8207–8213.
[64] S. Kaya, C. Kaya, A new equation for calculation of chemical hardness of groups and molecules, Molecular Phys 113 (11) (2015) 1311–1319.
[65] S. Kaya, C. Kaya, A new method for calculation of molecular hardness: a theoretical study, Comp. and Theo. Chem. 1060 (2015) 66–70.
[66] T.K. Ghanty, S.K. Ghosh, Correlation between hardness, polarizability, and size of atoms, molecules, and clusters, J. of Physical Chem. 97 (19) (1993) 4951–4953.
[67] R.G. Pearson, Hard and soft acids and bases, J. American Chem. Soc. 85 (22) (1963) 3533–3539.
[68] A. Asghar, M.M. Bello, A.A.A. Raman, W.M.A.W. Daud, A. Ramalingam, S.B.M. Zain, Predicting the degradation potential of Acid blue 113 by different oxidants using quantum chemical analysis, Heliyon 5 (9) (2019) e02396.